THE INTERNATIONAL JOURNAL OF MEDICAL ROBOTICS AND COMPUTER ASSISTED SURGERY
Int J Med Robotics Comput Assist Surg 2011; **7**: 85–95.
Published online 10 January 2011 in Wiley Online Library (wileyonlinelibrary.com) **DOI:** 10.1002/rcs.373

ORIGINAL ARTICLE

Noninvasive ultrasonic measuring system for bone geometry examination

K. Krysztoforski[1]
P. Krowicki[1]
E. Świątek-Najwer[1]*
R. Będziński[1]
P. Keppler[2]

[1]*Division of Biomedical Engineering and Experimental Mechanics, Institute of Machine Design and Operation, Wroclaw University of Technology, Poland*

[2]*Chirurgische Klinik Safranberg, Zenturm für Chirurgie, Klinik für Unfall-, Hand-, Plastische und Wiederherstellungschirurgie, Steinhövelstrasse 9, 89075 Ulm, Germany*

*Correspondence to:
E. Świątek-Najwer, Division of Biomedical Engineering and Experimental Mechanics, Institute of Machine Design and Operation, Wroclaw University of Technology, Lukasiewicza Str. 7/9, PL 50-371 Wrocław, Poland.
E-mail: ewelina.swiatek-najwer@pwr.wroc.pl

Accepted: 6 December 2010

Abstract

Background Bone deformities are typically identified through standard radiograms. Since X-ray examinations are easily applied and offer high quality imaging, noninvasive techniques are not commonly used in bone diagnostics. Nevertheless, nonradiological techniques are considered necessary because of the harmful effects of X-ray radiation.

Methods The paper presents a new noninvasive system for bone imaging. The system allows the physician to create self-defined templates of the measured geometrical parameters and to measure the bone geometry according to the planned procedures.

Results The proposed system was verified by determining the fiducial location error, the fiducial registration error and the target registration error. The tests were performed on sawbones and a measuring plate. In order to verify the accuracy of reconstruction, tests on the three-dimensional phantoms were carried out. The system has been tested in clinical conditions: results of limb geometrical parameters measured on five probands were compared with MRI-based evaluation.

Conclusions The system supplies critical data supporting the standard radiological examination. In the future, after further improvements it may replace invasive X-ray imaging. The main advantage of ultrasonography is noninvasive imaging (using mechanical waves), however, it demands considerable experience.

Keywords bone deformities; radiological investigation; noninvasive ultrasound bone imaging; error measurements

Introduction

Bone deformities are orthopaedic abnormalities that can be caused by congenital conditions, by abnormal growth or by healing in a deformed position after a bone fracture. Such deformities often manifest themselves in limb length discrepancies. Irregular shapes can be described as angulations, rotations and translations. The different irregularities sometimes occur at the same time. The treatment is corrective osteotomy, often supported by external or internal fixation applied to stabilize the bone components. When an external spatial frame protecting the internal tissues against injury is used, the treatment can be administered gradually (1).

Deformities affecting biomechanical conditions need to be described precisely in order to design a surgical scenario for correcting them. Standard radiographs in the anterior–posterior and lateral views are typically used in the diagnostic procedure. However, using two-dimensional views it is usually difficult to determine the nature of such deformities. Three-dimensional reconstruction of the bone shape and three-dimensional location of anthropometrical points and the bone axes provide a full description of the deformity conditions. Therefore three-dimensional computed tomography is the recommended imaging technique for diagnosing complicated deformities. However, so far noninvasive bone imaging techniques have not gained popularity in clinical practice. The reason is the high quality of X-ray scans (particularly of X-ray computed tomography) and easy interpretation. Nevertheless, clinicians are interested in replacing harmful X-ray imaging with noninvasive techniques.

According to Siston (2) small mislocations of landmarks lead to significant errors in orientation of the anatomical coordinate system. Therefore, percutaneous palpation used to adress landmarks, such as the symphysis pubis to define the anterior pelvic plane for referencing cup position in total hip arthroplasty, is not sufficiently precise (3).

Efforts are continuing to limit radiation when a patient undergoes computed tomography, nevertheless application of totally noninvasive equipment would solve the problem completely. Application of a sonographic technique for spatial measurements is a challenge in terms of image quality, precision and identification. Important disadvantages of sonography are artefacts introduced inter alia by reverberations and the assumption of constant ultrasound velocity. The first work on three-dimensional sonography concerned control of the ultrasound probe movement in a defined coordinate system, in which the probe was translated along an axis and the probe position read on a ruler (4). However, the construction was inconvenient for real measurements on a patient. Nowadays work on three-dimensional sonography applied in computer aided surgery considers acquisition of data to create statistical shape models. Advanced work concerns compensation for the influence of differences in speed of sound in different media (tissues) (3). Other applications of free-hand ultrasound imaging are intra-operative palpation of landmarks (5,6), registration of CT-data sets (7) or registration of bone echo points to CT-derived statistical shape models (8,9).

Application of ultrasound imaging techniques in clinical conditions has been described by Keppler *et al.*, who performed ultrasonic measurements of lower limb geometry on a representative group of patients. The results demonstrate the good repeatability and high precision of such measurements (10).

This paper presents a newly developed bone measuring free-hand sonographic system.

Material and Methods

Idea of the system

The noninvasive system for measuring bone geometry consists of an ultrasonographic probe with an infrared sensor mounted on it to track its position with an infrared camera. The free-hand sonographic system developed enables measurements of tissue geometry according to self-defined templates and semiautomatic shape reconstruction. The system has been applied in virtual planning of bone correction and intra-operative navigation of surgical instruments.

The free-hand ultrasonographic system (Figure 1) incorporates a Polaris Optical Tracking System (Northern Digital Inc., Canada) and a portable ultrasound system EchoBlaster 128 (Telemed, Lithuania). The software was developed in Microsoft Visual C++ 6.0, using the OpenGL standard specification to handle 3D computer graphics and the DirectShow technology for video stream control (11,12). The navigation system's field of view has a pyramid volume with a width of 1556 mm, a height of 1312 mm and a maximum distance of 2400 mm.

The navigation system sends the translation and the quaternion (defining the rotation) between the camera coordinate system and the coordinate system of any visible sensor. The latter can be mounted on the patient's body (transformation matrix B in Figure 2), the ultrasound probe (transformation matrix A in Figure 2) or on any navigated tool. The dynamic reference frame is mounted on blood arrest band which is noninvasively spread on the skin of shank. (13) The coordinate system transformation algorithms relate the ultrasound probe position to the patient coordinate system whereby any movements of the patient or the navigation system become insignificant.

The free-hand system allows one to analyze the three-dimensional shape of tissues without using any mechanical devices to control the movement of the ultrasound probe. The probe and sensor need to be calibrated to determine the calibration matrix defining the

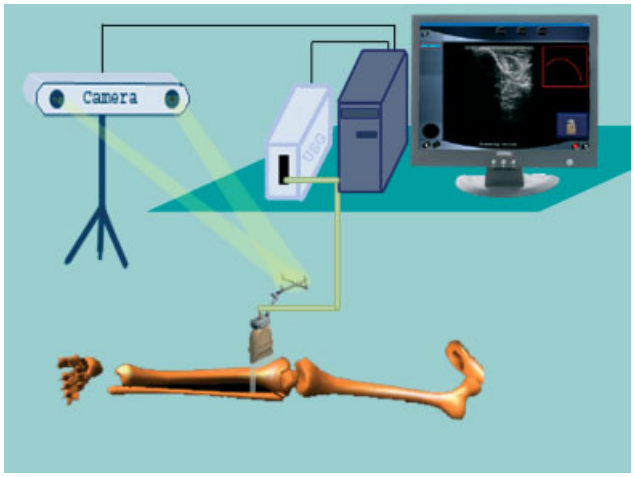

Figure 1. System for noninvasive bone measurements

DOI: 10.1002/rcs

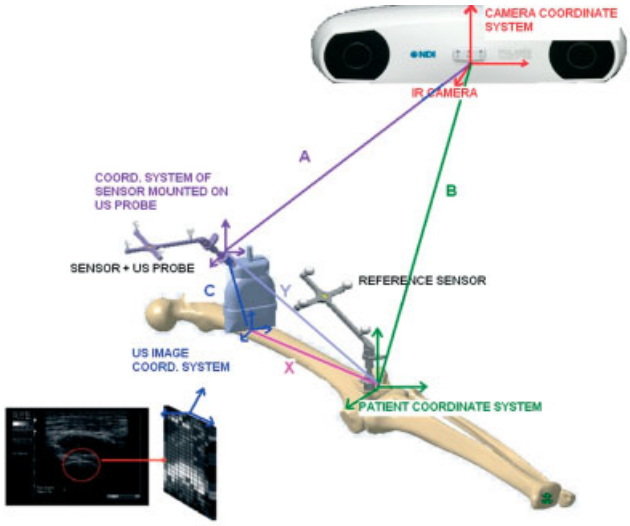

Figure 2. Transformation matrices

offset and rotation between the probe sensor coordinate system and the ultrasound image coordinate system (matrix C in Figure 2). The calibration matrix is needed to calculate the locations of ultrasound image pixels in the patient coordinate system.

The system is a universal bone measuring system. Measuring procedure templates are created on a virtual human skeleton by the physician. Such interaction with the surgeon is a new approach to bone geometry measurements. The application enables both the measurement of geometrical bone parameters and the reconstruction of the 3D shape of a bone surface. A flowchart of the system is shown in Figure 3.

Templates to measure geometrical parameters

In order to define a measurement templatethe user defines the location of the virtual probe in relation to the virtual skeleton. For probe location the application provides visualization of the approximate contour of the bone. For each virtual scan the user can define the position of landmarks; points, middle points, centres of circles, and vectors. The defined landmarks are visualized on a 3D bone model in the next application window. One can define lengths and angles between vectors, lengths and planes, and between a plane and a length. In order to define more complicated parameters the user can merge points, design a plane and project a point onto a plane. An example procedure for creating a femur length measurement template is shown in Figure 4.

Real measurement

The designed parameters can easily be measured. The user acquires scans and defines the position of the landmarks (Figure 5). The system visualizes the bone contour on the screen, which enables the physician to adjust the position of the probe. Once the data have been collected, the application displays the calculated parameters.

Bone shape identification

The proposed system offers the possibility of identifying the shape of a bone structure. The module consists of three parts: registration of scans, identification of bone contours in the scans and reconstruction of the spatial shape of the bone surface. The analysis of ultrasonographic images is a complicated and time-consuming process, involving the use of algorithms such as deformable models, neural networks and fuzzy clustering (14,15). In the system developed a Laplace gradient mask and median filtration are used in the pre-processing approach.

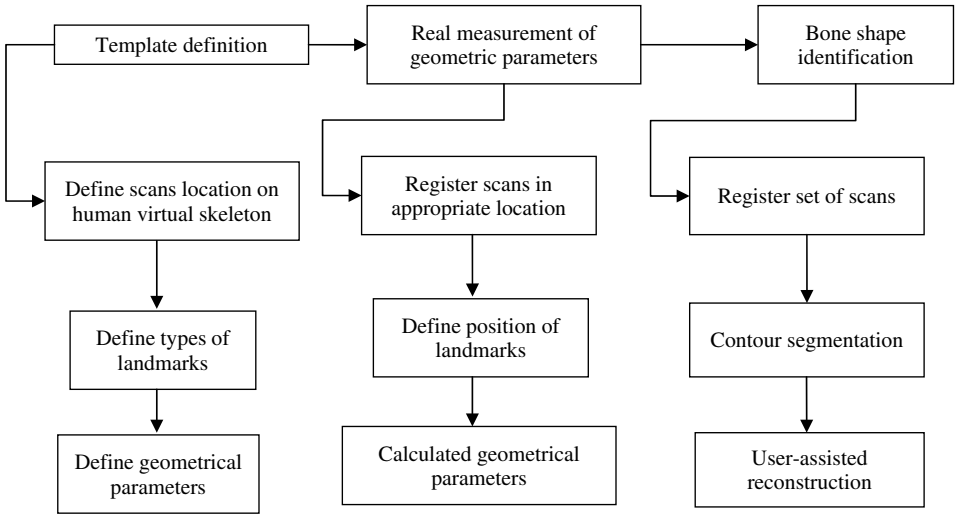

Figure 3. Modules of application

DOI: 10.1002/rcs

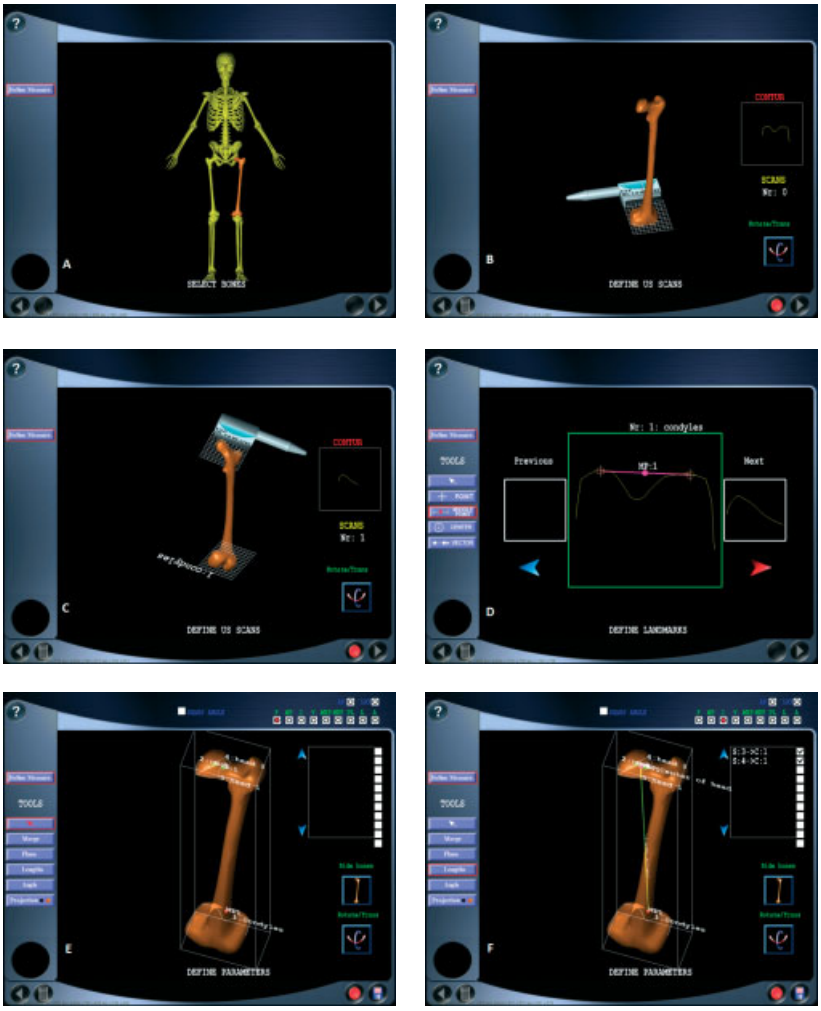

Figure 4. Definition of femur length measuring procedure template: (A) selection of bone (femur); (B) definition of probe position and virtual scan of condyles; (C) virtual scan of femur head; (D) definition of landmark (middle point between condyle points); (E) definition of length between femur head centre and knee centre; (F) 3D visualization of defined femur length

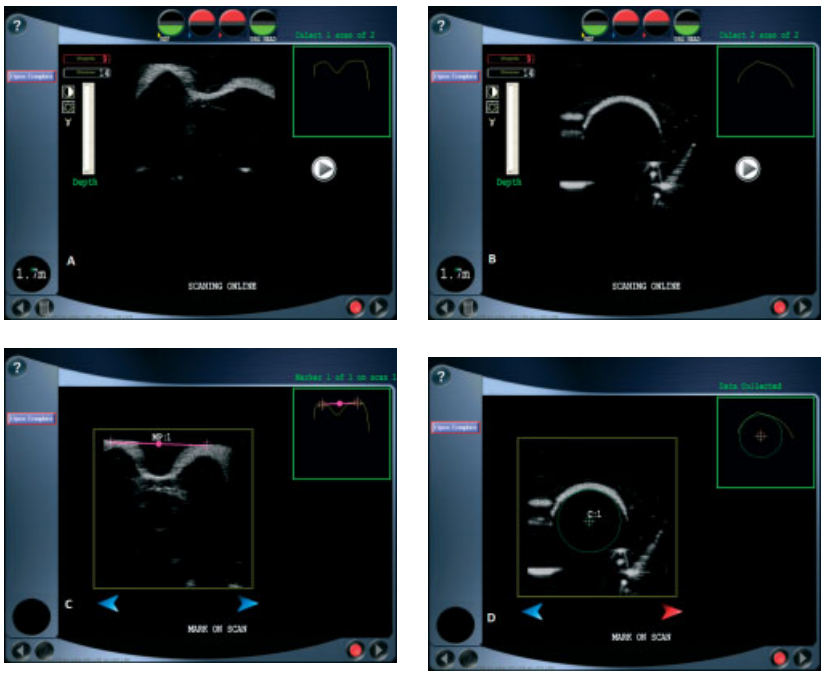

Figure 5. Measurement of femur length: (a) ultrasound scan of condyles; (b) ultrasound scan of femur head; (c) indicating landmarks (centre of knee); (d) indicating landmarks (centre of femur head)

DOI: 10.1002/rcs

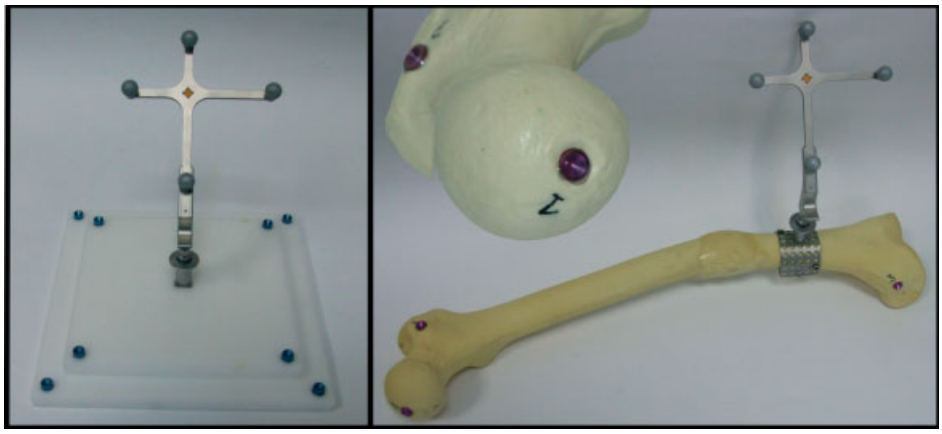

Figure 6. Measuring plate and one sawbone with mounted cones and reference rigid body

A knowledge of the physics of bone tissue ultrasonic imaging is exploited to determine the contour. It is well known that bone structures show higher acoustic impedance ($(3.65–7.09) \times 10^6$ kg/m^2/s) than soft tissues (1.63×10^6 kg/m^2/s) so that a hyper-echoic contour is received from the interface between them. Due to their high absorption rate (about 10 dB/cm/MHz) bones block ultrasound waves (16). For comparison, the absorption rate for soft tissues is less than 2 dB/cm/MHz. The findings concerning the strong echo from the bone–soft tissue interface and the anechoic structures under the contour are exploited in the analysis of the contour. The software provides a graphical interface for defining the region where an echo from the bone occurs. In the defined region the contour is searched from bottom to top.

The cloud of contour points determined from all the registered scans is used to reconstruct the shape. The reconstruction algorithm is semiautomatic. The application interface allows one to design the position of a plane, which is crucial for the reconstruction algorithm. The normal vector of the plane defines the direction of the projection of the points onto the visualized plane. The projected points are the input parameters for two-dimensional Delaunay triangulation. The algorithm designs the connection of the points into triangles, then it defines the connections between three-dimensional points. Finally, the points are connected into triangles and the normal vector is calculated for each triangle.

Tests of accuracy

The method of testing accuracy by applying fiducials is a standard technique in the primary evaluation of imaging systems (4,13). Obviously, fiducials are easily interpreted on the image, in contrast to real tissues; however, even in the case of metal cones, one must be aware of artefacts, which can be eliminated by proper positioning of the ultrasound probe. The accuracy of tissue examination has been evaluated by comparison of geometrical parameters obtained using the proposed ultrasound system with those obtained by MRI analysis.

Test of fiducial location error (FLE), fiducial registration error (FRE) and target registration error (TRE)

Tests were performed to validate the accuracy of the navigator using a measuring plate containing eight easily palpable cones with a basis radius of 0.7 mm (Figure 6). The measuring plate was tested using a Zeiss coordinate machine to determine the precise positions of each cone fovea in the coordinate system of a rigid body mounted 'on-plate'.

To check the accuracy of the localizer itself a navigated pointer was used. The coordinates obtained were related to those measured by the Zeiss coordinate machine. The FLE error was calculated as an RMS value from the equation:

$$FLE = \sqrt{\frac{1}{n}\sum_{i=1}^{n}(x_i - \bar{x})^2}$$

where n is the number of measurements, x_i is the measured coordinate and $\bar{x}$ is the 'true' coordinate value measured by the Zeiss machine.

In order to determine the FLE (influenced by both the navigation system error and the analysis of sonographic scans), measurements were performed on three sawbones with six mounted cone foveae (Figure 6), with the sawbones placed in a water basin. The positions of the foveae visualized in ultrasound scans were calculated in the coordinate system of the rigid body mounted on the sawbone. The coordinates determined for the cones foveae were related to the positions reached by the navigated pointer during palpation.

The identified positions of the cones foveae and the positions determined by palpation with the navigated pointer were used to evaluate the FRE. The positions of the foveae visualized in the ultrasound scans were calculated in the coordinate system of the rigid body mounted on the sawbone. Then palpation with the navigated pointer was performed.

DOI: 10.1002/rcs

The reference coordinate system was placed in a different location to that for the ultrasonic measurements to reflect the circumstances of pre-operative and intra-operative procedures. On the basis of four of the six points measured in the two coordinate systems a matching matrix was calculated using the Landmark Transform algorithm from the Visualization Toolkit (VTK). The transform matrix is defined by two sets of landmarks and the computed transform gives the best least squares mapping. In order to calculate the FRE, the coordinates of the points registered in the ultrasound scans (the ultrasound coordinate system), which had been used in the matching procedure, were transformed using the calculated matching matrix to get related points in the second coordinate system (connected with the palpation process).

The FRE represents the registration procedure accuracy expressed as a distance between the calculated coordinates of the points and the original (desired) coordinates measured during the palpation procedure. The coordinates of the control points not considered during the matching procedure were taken into account to calculate the TRE. The latter represents the error of intra-operative ultrasound image-aided navigation

Test on ultrasound calibration phantom

A three-dimensional ultrasound calibration phantom made by CIRS was used to test the accuracy of the measuring system. The phantom contains two calibrated volumetric test objects. The phantom is made of Zerdine™ – a solid elastic water-based polymer with an attenuation coefficient 0.5 dB/cm/MHz ±0.05 dB/cm/MHz.

The shape of the volumetric objects is ellipsoidal (Figure 7). The intersections are circles with changing radii. One of the large circle and two of the smallest circles visible at the two ends are registered. The locations of the centres of the three circles were calculated and the ellipsoid axes have been estimated. Finally, reconstruction of the smaller object has been performed. The volume of the calibrated object has been estimated, and calculated based on the formula for an ellipsoidal object.

Tests of reconstruction procedure

To test the influence of shape complexity on the results of the modelling algorithm three femur sawbones were reconstructed. The value of the error is the average distance between points addressed by the navigated pointer to the nearest triangle of the reconstructed mesh.

Clinical tests

To test the system in clinical conditions five volunteer probands were subjected to magnetic resonance imaging and study using the proposed system. To test lower limb length, femur length and three-dimensional collodiaphyseal angle the following scans were recorded: femur head (three scans of various intersections), condyles, distal epiphysis of tibia, neck and femur shaft (17).

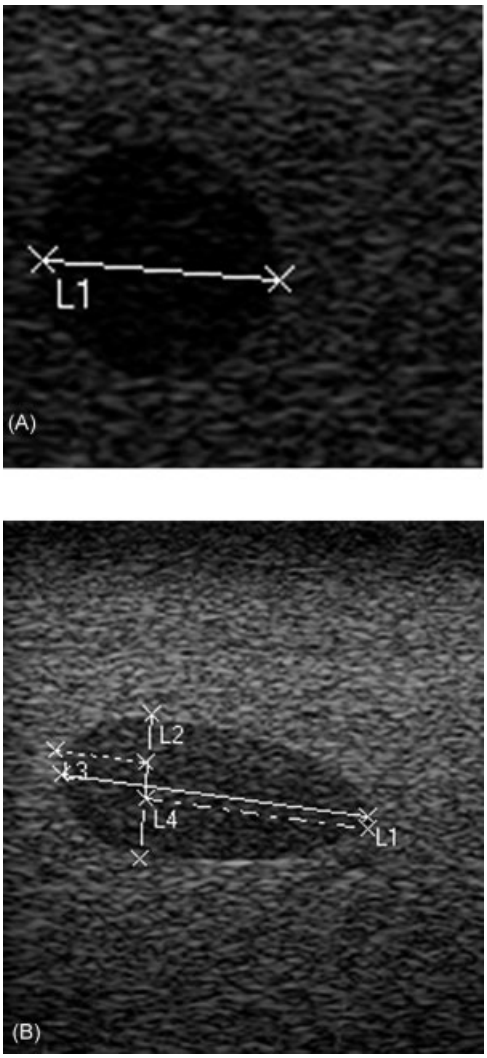

Figure 7. Scan of volumetric object: intersection is a circle and ellipse

Results

Results of tests of FLE, FRE and TRE

The FLE describing the accuracy of navigation system in three directions (x,y,z) is given by $FLE(N)_x$, $FLE(N)_y$, $FLE(N)_z$. The average FLE describing the accuracy of fiducial identification in three directions (x,y,z) is $FLE(U)_x$, $FLE(U)_y$, $FLE(U)_z$, $FLE(U)_{3D}$. The values are presented in Table 1.

Table 1. Results of FLE measurements

Type of error	Magnitude (mm)
$FLE(N)_x$	0.31 ± 0.14
$FLE(N)_y$	0.58 ± 0.13
$FLE(N)_z$	0.32 ± 0.16
$FLE(U)_x$	1.51 ± 1.28
$FLE(U)_y$	2.02 ± 1.08
$FLE(U)_z$	2.03 ± 1.07
$FLE(U)_{3D}$	3.24 ± 1.98

Table 2. Results of FRE and TRE measurements

Phantom	FRE (mm)	TRE (mm)
1	1.35 ± 0.15	2.24 ± 0.10
2	1.38 ± 0.30	2.41 ± 0.45
3	0.89 ± 0.38	2.05 ± 0.73

Table 2 presents results of FRE and TRE evaluated on three sawbones.

Results of test on ultrasound calibration phantom

The nominal 'true' dimensions of the volumetric objects are shown in Figure 8.

The test was repeated 10 times. The length of the longer axis differs from the 'true' value by less than 1 mm (Table 3, Figure 9). The deviation in the case of the shorter axis length measurement was due to the imprecise positioning of the large circle (Table 3, Figure 10).

Visualization of the cloud of points and the reconstructed shape of the calibrated object are shown in Figure 11. The measured long and short axes of the ellipsoid were used to calculate the volume from the equation

$$Volume = \frac{4}{3}\pi \times \frac{A_1}{2} \times \left(\frac{B}{2}\right)^2 + \frac{4}{3}\pi \times \frac{A_2}{2} \times \left(\frac{B}{2}\right)^2$$

where A_1 is the short half of the long axis, A_2 is the long half of the long axis, and B is the short axis.

The calculated volume was 6.45 cm^3, whereas using the 'true' values of the ellipsoid axes gives a volume of 6.62 cm^3. The accuracy of the volume depends on the accuracy with which the long and short axes are determined. The manufacturer-calibrated volume of the object was 7.10 cm^3. The reconstruction was repeated for 28 scans registered on the same phantom surface. 118 bone contour points were connected into 232 triangles. The data were loaded into the MIMICS Materialise software which can calculate various parameters for a

Table 3. Results of tests on three-dimensional phantom

Parameter	Mean measured value (mm)	Nominal value (mm)
Longer axis length	38.04 ± 0.78	39.0
Shorter axis length	15.58 ± 1.03	18.0

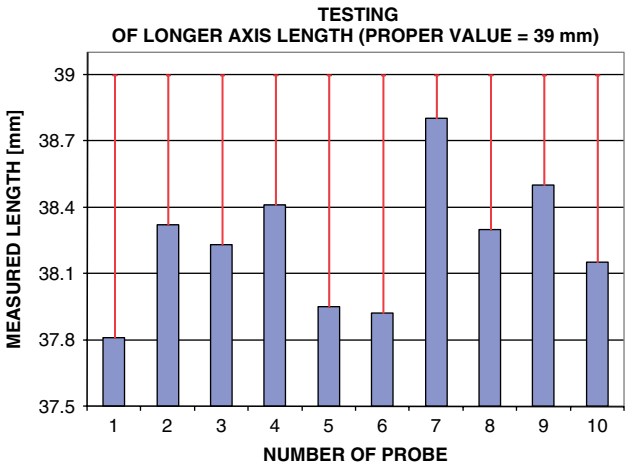

Figure 9. Results of measurement of volumetric object's longer axis

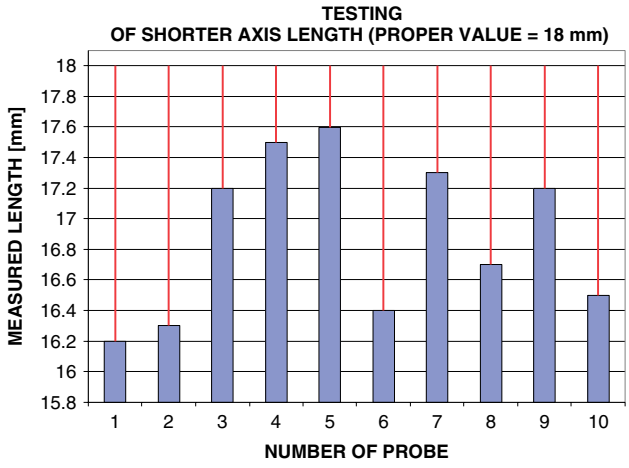

Figure 10. Results of measurement of volumetric object's shorter axis

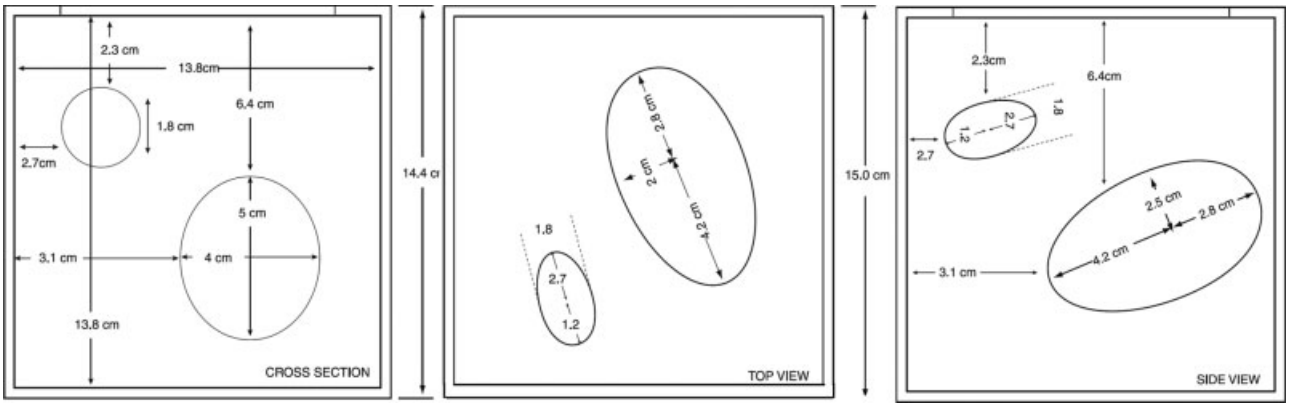

Figure 8. Nominal proper dimensions of volumetric objects (18)

DOI: 10.1002/rcs

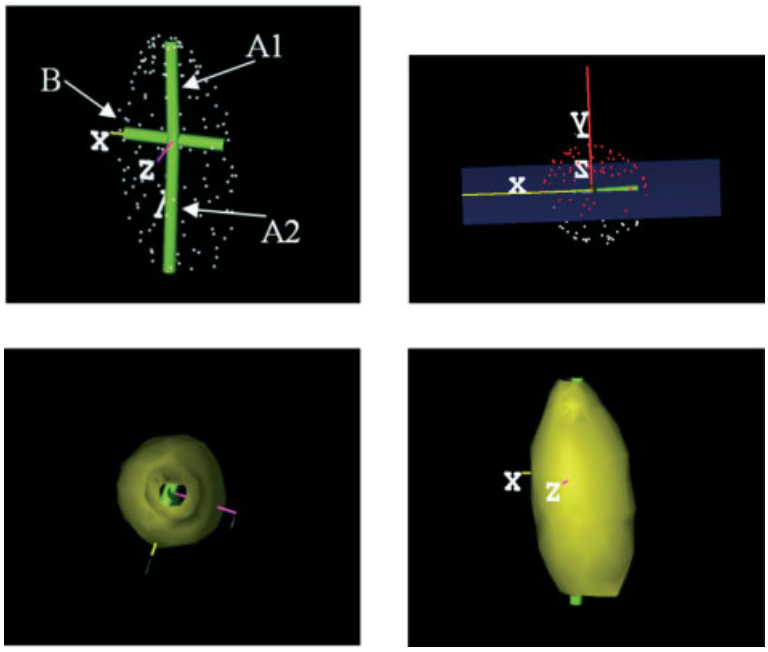

Figure 11. Volumetric object reconstruction: (a) cloud of points; (b) reconstruction procedure; (c) 3D views of reconstructed object

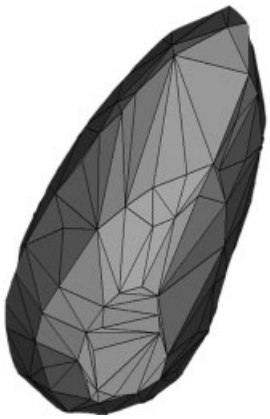

Figure 12. Volumetric object reconstruction by means of MIMICS Materialise software

given mesh. One such parameter is the volume of the closed surface. The volume was 7.03 cm^3 (Figure 12), a deviation from the real value of 0.07 cm^3.

Since the calibrated object is not ideally ellipsoidal in shape its volume differs from the volume calculated using the calibrated axes of the "ellipsoid". The respective volumes agree well with the measurements.

Results of tests of reconstruction

Results of tests of the reconstruction of three regions of the femur sawbone (head, shaft and condyles) are shown in Figure 13 and Table 4.

The condyles and head are the most complex shapes, even in the case of deformity, and the accuracy of their reconstruction is about 2 mm.

The accuracy of phantom reconstruction depends only on the accuracy of the system; human interaction affects are insignificant because of the high contrast echo of the object. However, when tissue is investigated, it is crucial to define the contour of the bone real echo because of its considerable width. It was decided to determine the direction of bone echo searching – downwards – first pixels of the acoustical shadow, or upwards – first pixels of the high intensity echo. Human interaction is necessary during modelling, where the projection plane is defined and the reconstruction is performed in a step by step procedure. The acquisition of scans needs to be carefully considered, because the more densely the scans are recorded the higher the resolution of the shape. The resolution determines whether the deformation of the bone is revealed in the reconstructed object. The other important requirement, typical in ultrasonography, is proper positioning of the probe to achieve a high contrast echo. The reconstruction procedure requires user experience in bone sonography and modelling.

The deformity itself does not influence the accuracy of reconstruction, since the reconstruction is based only on recorded scans. The reconstruction method is efficient for any set of points of both deformed and straight bone surface. However, complex shapes are prone to greater errors in reconstruction if the scans are recorded at a greater distance.

Results of clinical tests

The example scans recorded to identify landmarks and to evaluate geometrical parameters are presented in Figure 14.

The results of comparative analysis of femur length measured using sonography and magnetic resonance imaging are presented in Figure 15.

DOI: 10.1002/rcs

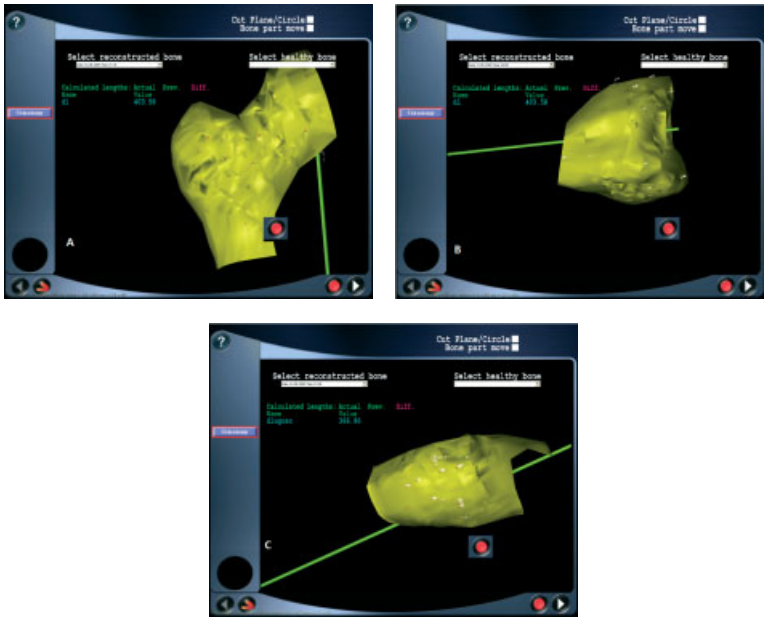

Figure 13. Results of ultrasound-based reconstruction of three regions of femur synbones (A – head, B – condyles and C – shaft)

Table 4. Results of tests of reconstruction of sawbones

Reconstructed region	Error value (mm)
shaft	0.41 ± 0.34
head	2.22 ± 0.43
condyles	1.26 ± 1.11

The comparative analysis revealed a high Pearson's correlation coefficient of 0.99 between appropriate parameters. The deviations between MRI- and sonography-based parameters were estimated at 0.42–4.33 mm. For the collodiaphyseal angle the deviation was estimated at 2.5°.

Discussion

The aim of this work was to develop a system for noninvasive measurements of bone tissue and virtual planning of sonography-based reconstructed models in order to reduce radiation exposure in pre-operative and intra-operative stages.

The system for noninvasive measurements of bone shape has a precision expressed by the average TRE of 2 mm. The resolution of the ultrasound probe depends on the frequency (5 MHz) and the penetration depth (80 mm). The sonographic image pixel size is 0.156 mm.

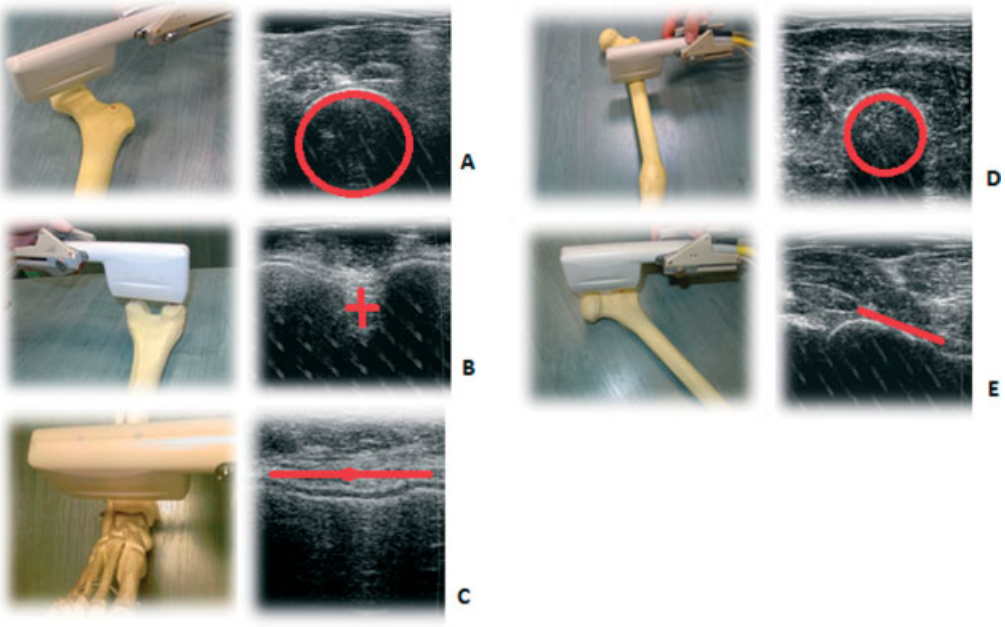

Figure 14. Location and view of ultrasound scans of lower limb (A – femur head, B – condyles, C – distal epiphysis of tibia, D – shaft, E – neck)

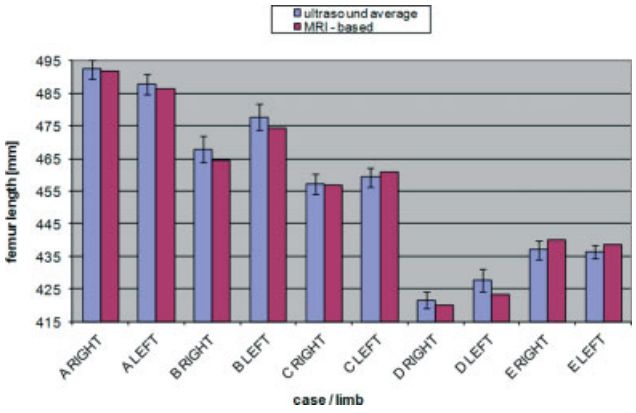

Figure 15. Results of comparative analysis of ultrasound to MRI-based measurements of femur length

The system is a universal tool for identifying the geometry of bones. The parameters can be defined by the user and the graphical interface provides a better understanding of the design procedures.

An important problem raised by clinicians is that the parameters in ultrasonic scans are not the same as the parameters defined in standard radiographs. The problem can be easily solved by, for example, projecting the parameters onto the frontal plane defined by the position of landmarks. The definition of three-dimensional parameters, although complicated, provides a full description of disorders and so the analysis should not be limited to two dimensions.

In ultrasound systems the quality of images poses a problem. The main solution is to use advanced filtering algorithms, which, however, are time-consuming and not necessarily error-free. Artefacts in ultrasound images result in difficulties for the automatic analysis of the images. Although ultrasonic imaging enables identification of the echo received from the bone structure, the region of interest still needs to be defined and so any algorithm requires assistance from the user.

FLE, FRE and TRE values show that the system accuracy is reasonably high. The main factors affecting the results are the localizer error and inaccurate identification of the cone foveae on the ultrasound screen. Also the probe resolution (determined by the ultrasound frequency) and artefacts introduced by reverberations (occurring at a specific angle of the probe to the object) affect analysis of the sonographic scan. Nevertheless, the accuracy (as expressed by the TRE) is acceptable for a system that is a noninvasive and less expensive alternative to CT-based measurements.

The system presented can be used by clinicians experienced in ultrasound techniques. The results of tests carried out on phantoms show that the system accuracy and repeatability are adequate for bone geometry measurements. One should note that in tests performed on the calibration phantom the echo from the interface between materials with different impedances is weak. In real bone tissue measurements the strength of the echo depends on the pressure exerted by the probe on the skin and on the incidence angle of the ultrasound. Echo strength is crucial for the identification of bone surfaces. However, comparative analysis of results of clinical tests on probands with results of MRI-based measurements revealed strong correlation and small deviations. This has encouraged the authors to continue clinical tests in the near future and to improve algorithms for tissue identification from the ultrasound dataset.

Acknowledgements

This work was supported by grant No. N R 13 0012 04 given by National Centre of Research and Development in Poland, and National Cohesion Strategy, Regional Strategy of Innovation: 'Grant – support for research by scholarship for PhD students'.

References

1. Paley D. *Principles of Deformity Correction*. Springer-Verlag: Berlin/Heidelberg/New York, 2002.
2. Siston RA, Giori NJ, Goodman SB, Delp SL. Surgical navigation for total knee arthroplasty: a perspective. *J Biomech* 2007; **40**: 728–735.
3. Schumann S, Puls M, Ecker T, Schwaegli T, Stifter J, Siebenrock KA, Zheng G. Determination of pelvic orientation from ultrasound images using patch-SSMs and a hierarchical speed of sound compensation strategy. In *IPCAI 2010: Proceedings of the 1st International Conference on Information Processing in Computer-Assisted Interventions*, 23 June 2010, Geneva, Switzerland, Navab N, Jannin P (eds). Springer-Verlag: Berlin/Heidelberg, 2010; 157–167.
4. Young DI, Staniforth SM, Hu RW. Three-dimensional measurement of the femur using clinical ultrasound: developing a basis for image guided intramedullary nail fixation of the femur. In *MICCAI 2000: Proceedings of the 3rd Medical Image Computing and Computer-Assisted Intervention*, 11–14 October 2000, Pittsburgh, USA, Delp SL, DiGioia AM, Jaramaz B (eds). Springer-Verlag: Berlin/Heidelberg, 2000; 1220–1228.
5. Admin DV, Kanade T, DiGioia AM, Jaramaz B. Ultrasound registration of the bone surface for surgical navigation. *Comput Aided Surg* 2003; **8**(1): 1–16.
6. Kozak J, Wehrle Ch, Wittek M, Keppler P. Semi automated and noninvasive determination of bone landmarks using a navigated US. In *CAOS 2005: Proceedings of the 5th Annual Meeting of International Society for Computer Assisted Orthopaedic Surgery*, 19–22 June 2005, Helsinki, Finland, Langlotz F, Davies BL, Schlenzka D (eds); p. 258.
7. Brendel B, Winter S, Rick A, Stockheim M, Ermert H. Registration of 3D CT and ultrasound datasets of the spine using ultrasound bone structures. *Comput Aided Surg* 2002; **7**(1): 146–155.
8. Chan CSK, Barratt DC, Edwards PJ, Penney GP, Slomczykowski M, Carter TJ, Hawkes DJ. Cadaver validation of the use of ultrasound for 3d model instantiation of bony anatomy in image guided orthopaedic surgery. In *MICCAI 2004: Proceedings of the 7th Medical Image Computing and Computer-Assisted Intervention*, 26–30 September 2004, Rennes Saint-Malo, France, Barillot C, Haynor DR, Hellier P (eds). Springer-Verlag: Berlin/Heidelberg, 2004; 397–404.
9. Rajamani KT, Styner MA, Talib H, Zheng G, Nolte LP, González Ballester MA. Statistical deformable bone models for robust 3D surface extrapolation from sparse data. *Med Image Analysis* 2007; **11**: 99–109.
10. Keppler P, Strecker W, Kinzl L, Simmnacher M, Claes L. Die sonographische Bestimmung der Beingeometrie. *Orthopaede* 1999; **28**: 1015–1022.

11. Keppler P, Krysztoforski K, Swiatek-Najwer E, Krowicki P, Kozak J, Gebhard F, Pinzuti JB. A new experimental measurement and planning tool for sonographic-assisted navigation. *Orthopaedics* 2007; **30**(10): 144–147.
12. Krowicki P, Swiatek-Najwer E, Keppler P, Kozak J, Krysztoforski K. Bone reconstruction based on sonography and data acquired from tracking system. In *CAOS 2007: Proceedings of the 7th Annual Meeting of International Society for Computer Assisted Orthopaedic Surgery*, 20–23 June 2007, Heidelberg, Germany, Langlotz F, Davies BL, Gruetzner PA (eds). Verlag Pro Business: Berlin, 2007; 646–647.
13. Kozak J, Mairaj D, Krupakaran N, Keppler P. Evaluation of noninvasive referencing for navigated ultrasound registration in pre-. intra-. post-operative procedures. In *CAOS 2007: Proceedings of the 7th Annual Meeting of International Society for Computer Assisted Orthopaedic Surgery*, 20–23 June 2007, Heidelberg, Germany, Langlotz F, Davies BL, Gruetzner PA (eds). Verlag Pro Business: Berlin, 2007; 282–284.
14. Bankman I. *Handbook of Medical Imaging. Processing and Analysis*. Academic Press: San Diego, 2000.
15. Russ JC. *The Image Processing Handbook*. CRC Press/Taylor and Francis Group: Boca Raton, 2007.
16. Daanen V, Tonetti J, Troccaz J. An Information Fusion Method for the Automatic Delineation of the Bone-Soft Tissues Interface in Ultrasound Images. In *CVAMIA-MMBIA 2004. Proceedings of the Mathematical Methods in Biomedical Image Analysis and Computer Vision Approaches to Medical Image Analysis Workshop*, 15 May 2004, Prague, Czech Republic, Sonka M (ed). Springer-Verlag: Berlin/Heidelberg, 2004; 218–229.
17. Swiatek-Najwer E, Bedzinski R, Dragan SL, Krowicki P, Krysztoforski K. Investigation of lower limb mechanical axis using 3D sonography and magnetic resonance. In *Proceedings of 27th Danubia-Adria Symposium on Advances in Experimental Mechanics*, 22–25 September 2010, Wroclaw, Poland Wroclaw University of Technology Press: Wroclaw, 2010; 217–218.
18. The Spatial Measurement Phantom Task Group of the American Institute of Ultrasound in Medicine Technical Standards Committee. *Standard Methods for Calibration of 2-Dimensional and 3-Dimensional Spatial Measurement Capabilities of Pulse Echo Ultrasound Imaging Systems*. American Institute of Ultrasound in Medicine. ISBN: 1-930047-94-0.